DOI: 10.1002/ejoc.200800190

Solution Conformation and Dynamics of the O-Antigen of the Major Lipopolysaccharide from *Sinorhizobium fredii* SMH12

Francisco J. Fernández de Córdoba,[a] Miguel A. Rodríguez-Carvajal,*[a] Francisco J. Cañada,[b] Pilar Tejero-Mateo,[a] Antonio M. Gil-Serrano,*[a] and Jesús Jiménez-Barbero*[b]

Keywords: Conformation analysis / NMR spectroscopy / Molecular dynamics / Lipopolysaccharides / Antigens

The conformational and dynamic behavior of the O-antigen of the lipopolysaccharide of *Sinorhizobium fredii* SMH12, a wide-range host bacterium isolated from nodulated soybean plants growing in Vietnam, was studied. The O-antigen has a repeating unit consisting of the trisaccharide →4)-α-D-Gal*p*A-(1→3)-2-*O*-Ac-α-L-Rha*p*-(1→3)-2-*O*-Ac-α-D-Man*p*-(1→, where the O-6 position of the mannose residue in the repeating unit is unsubstituted, acetylated, or methylated in an approximate ratio 1:1:2. For the analysis of the conformational and dynamic behavior, the deacetylated polysaccharide was employed. A combination of NMR spectroscopic methods assisted by molecular mechanics and dynamic simulations was employed to deduce its major conformational and dynamic features.

Introduction

Sinorhizobium fredii SMH12 is a fast-growing Gram-negative soil bacterium that is able to enter into a nitrogen-fixing symbiosis with plants of the legume family,[1] such as *Glycine max* (soy bean). In addition to the Nod factors,[2] several rhizobial surface polysaccharides are necessary for successful nodulation, as they act as signal molecules and/or they prevent plant defense response.[3–5] The outer membrane of rhizobia is formed of proteins, lipopolysaccharides (LPSs), and phospholipids. In the genus *Sinorhizobium*, the outer membrane and the surrounding capsule are constituted in part by a complex array of lipopolysaccharides, capsular polysaccharides, and exopolysaccharides.

Within LPSs, the O-chain polysaccharide is a polymerized repeating oligosaccharide whose composition is highly variable in different rhizobia. This O-chain is responsible for the antigenic properties of the LPS (the so-called O-antigen). We recently showed that the fast-growing *Sinorhizobium fredii* SMH12, a wide-range host bacterium isolated from nodulated soybean plants growing in Vietnam, produces an LPS whose O-antigen has a repeating unit[6] consisting of the trisaccharide →4)-α-D-Gal*p*A-(1→3)-2-*O*-Ac-α-L-Rha*p*-(1→3)-2-*O*-Ac-α-D-Man*p*-(1→. Because the antigenic properties can be related to the spatial presentation of the O-antigen and, thus, to its conformational and dynamic properties, we have carried out a detailed study of these features by using a combined NMR/molecular dynamics (MD) protocol.[7] Although nowadays the existence of flexibility and dynamic motion around the glycosidic linkages of oligosaccharide molecules has been largely demonstrated,[8] the observed data unequivocally indicate the presence of distinct flexibility for the different glycosidic linkages, depending on the nature and relative stereochemistries of the attached sugars.[9]

[a] Department of Organic Chemistry, Faculty of Chemistry, University of Seville,
41012 Sevilla, Spain
E-mail: agil@us.es
rcarvaj@us.es
[b] Department of Protein Science, CIB-CSIC,
Ramiro de Maeztu 9, 28040 Madrid, Spain
E-mail: jjbarbero@cib.csic.es
Supporting information for this article is available on the WWW under http://www.eurjoc.org or from the author.

Results and Discussion

Figure 1a shows the conformational Φ/Ψ maps generated for the trisaccharide repeating unit of the deacetylated O-antigen polysaccharide. It can be observed that there are two well-defined conformational minima for the Man1→4GalA glycosidic linkage with Φ/Ψ values of ca. 20/40° and –50/–30°, whereas there is a very major orientation for both the Rha1→3Man (60°/40°) and GalA1→3Rha moieties (–50/–40°).

A representation of an octasaccharide structure taken from the combination of the major minima for the three glycosidic linkages is shown in Figure 2.

Then, a similar MD simulation was also performed for the native acetylated polysaccharide (by using an octasaccharide model) by using the global minimum of the deacetylated molecule. The corresponding conformational maps in terms of the Φ/Ψ angles for every glycosidic linkage are given in Figure 1b. The maps for both acetylated and de-

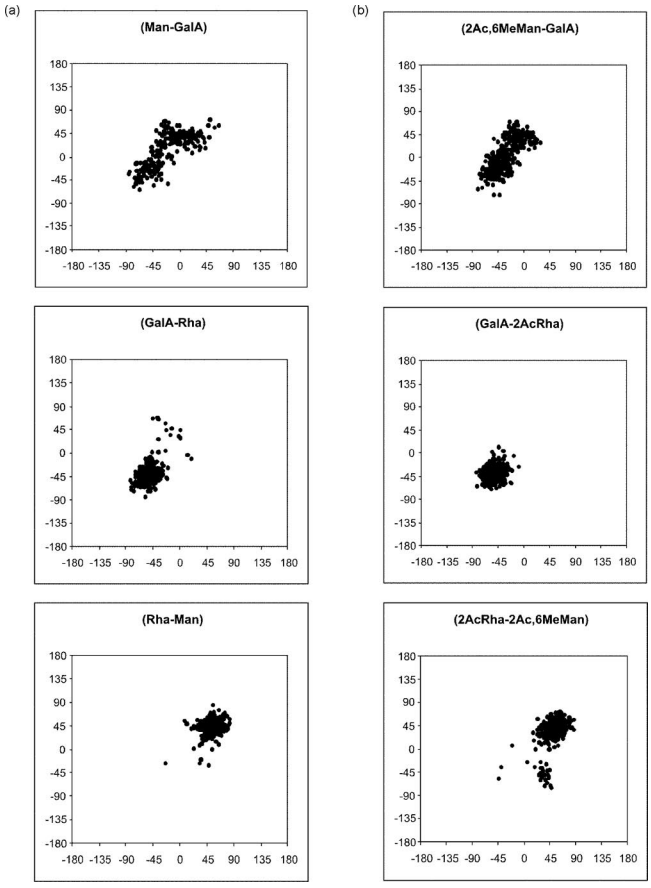

Figure 1. (a) Conformational maps Φ vs. Ψ for the Man1→4GalA (MG), GalA1→3Rha (GR) and Rha1→3Man (RM) glycosidic linkages of the deacetylated octasaccharide taken as a model for the O-antigen, as deduced from the MD simulations; (b) conformational maps Φ vs. Ψ for the Man1→4GalA (MG), GalA1→3Rha (GR) and Rha1→3Man (RM) glycosidic linkages of the native acetylated octasaccharide taken as model for the O-antigen, as deduced from the MD simulations.

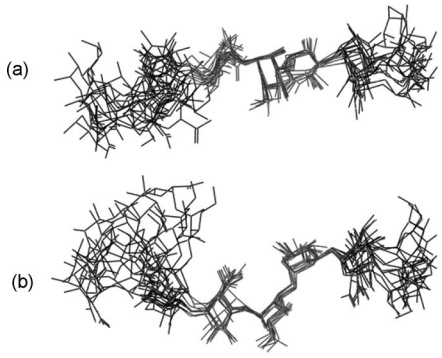

Figure 2. Superimposition of different conformers found during the MD simulation of the octasaccharide. (a) The glycosidic torsions for the Man1→4GalA linkage are $\Psi_{MG} < 0$; (b) the glycosidic torsions for the Man1→4GalA linkage are $\Psi_{MG} > 0$. The trisaccharide repeating unit is shown in light print.

acetylated molecules are indeed very similar in terms of the relative orientation of the different moieties and the extent of flexibility around the glycosidic linkages. Indeed, the axial orientation of the acetyl moieties places them almost perpendicular to the saccharide main chain, with no interactions with the contiguous residues. Thus, the deacetytaled molecule may be used as a model to study the conformational dynamics of the O-antigen (Figure 3).

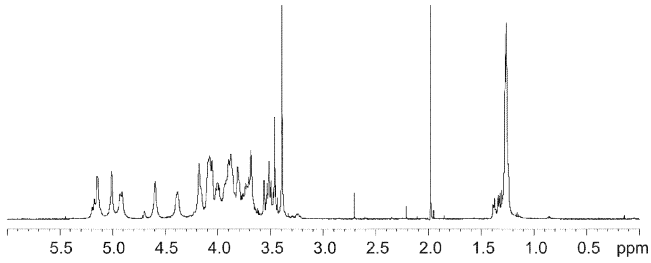

Figure 3. 500 MHz ^{1}H NMR of the deacetylated O-antigen after purification by size-exclusion chromatography.

NMR Spectroscopic Analysis

The validity of the conclusions taken from the MD simulations was assessed by using NMR spectroscopic data. In a first step, the NMR spectrum of the deacetylated polysaccharide was assigned by using a combination of standard 2D techniques. Assignments of ^{1}H and ^{13}C NMR spectra were made on the basis of DQF-COSY, multiplicity-edited HSQC (Figure S1, Supporting Information), coupled HSQC, TOCSY (Figure S2, Supporting Information), NOESY (Figure S2, Supporting Information), and HMBC experiments. All chemical shifts are summarized in Table S1 (Supporting Information). As the following step, the NOE cross peaks were integrated at the different mixing times, and their values were compared to those computed by application of a full-matrix relaxation approach[10] to the structures saved during the MD simulation of the octasaccharide model. The comparison of the data for the NOESY acquired with a mixing time of 150 ms with a variety of rotational correlation times is shown in Table 1.

The best fit values of the effective correlation times for the Man1→4GalA, GalA1→3Rha, and Rha1→3Man linkages are τ_C = 5.5, 9, and 16 ns, respectively. These values indicate that the different linkages show different degrees of flexibility. In fact, the Man1→4GalA linkage is the most flexible one, followed by the Gal1→3Rha analogue. According to the NOE data, the Rha1→3Man linkage is rather rigid. The comparison between the experimental and theoretical data was performed by using the geometries from the MD run, as well as an octasaccharide built from the averaged Φ/Ψ values, for the different glycosidic linkages. The fit was very similar independently of the employed model.

The different flexibility is also in agreement (at least qualitative) with the shape of the potential-energy surfaces.[11] Two different minima are clearly observed for the Man1→4GalA linkage, with sensibly distinct Φ/Ψ values (6/40° and –49/–23°). The NOE data indicate that both conformers contribute to the polysaccharide shape and, thus,

Table 1. Experimental and computed NOEs for a 2D-NOESY experiment (150 ms) recorded for the deacetylated O-antigen. The values between the anomeric 1-H proton of every residue and the key intra- and interresidual protons are shown. The shadowed values correspond to overlapped signals in the NOESY spectrum. The NOESY values from the MD simulation were calculated by using the MD-computed structures and by employing different effective correlation times for the 1-H–X-H proton pairs of the different residues (see text).

1-H (τ_C)[a]	NOE to	Experimental [%]	MD [%]
Man (5.5 ns)	2-H Man	22	18
	3-H GalA		4
	4-H GalA	29	30
	5-H GalA	3	4
GalA (9 ns)	3-H GalA	7	5
	2-H GalA	37	23
	3-H Rha		16
	2-H Rha	27	36
	1-H Rha	13	4
Rha (16 ns)	2-H Rha	37	35
	1-H GalA	16	12
	3-H Man	33	36
	2-H Man	22	8
	5-H Man		8

[a] Only the most-effective τ_C values that properly fit the NOEs are given in parentheses in the first column.

the degree of motion around the Man1→4GalA linkage is rather high. In contrast, only one main minimum is found for each of the other two Gal1→3Rha and Rha1→3Man disaccharide fragments. From the inspection of the potential-energy surfaces of the two entities, no major differences are foreseen, although the relative interresidual interactions are different in the two fragments, because of the different relative stereochemistries (D-Man vs. L-Rha).

In any case, as a result of its intrinsically large flexibility, the polysaccharide antigen would present a high degree of motion and, therefore, could modulate the presentation of distinct polar and nonpolar patches for interacting with the corresponding receptor molecule.

A view of an octasaccharide model of the polysaccharide in its more-stable conformation (with a negative Φ value for the Man1→4Gal linkage), as well as a view of its polar and nonpolar surfaces, is shown in Figure 4. The same information for the alternative Φ conformer is also given.

In conclusion, the analysis of the NMR spectroscopic and molecular mechanics data allows assessing the presence of different timescales for the motion of an antigenic polysaccharide. Although the presence of internal motion for saccharide glycosidic linkages is beyond discussion, the data gathered herein show, in a nonambiguous manner, this fact, as well as the presence of different motional regimes for the different glycosidic linkages of the molecules. Although merely speculative, the presence of these distinct motional timescales could be related to the biological response of this antigenic molecule.

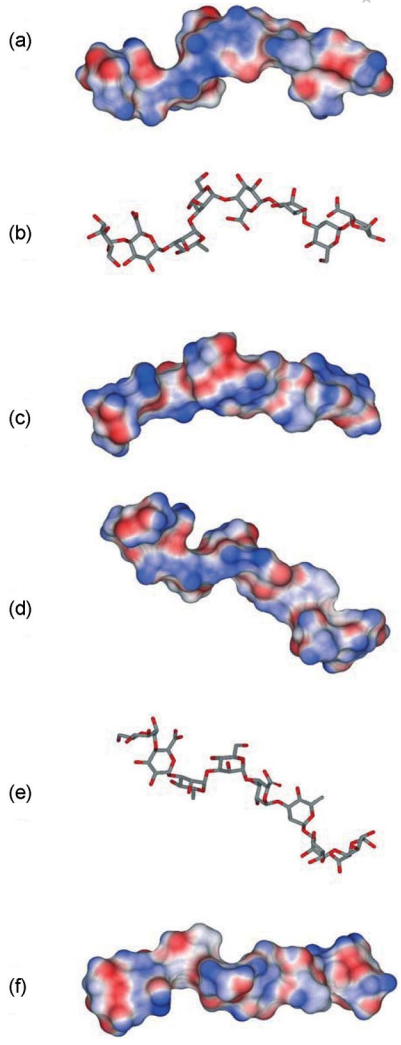

Figure 4. Presentation of an octasaccharide of the deacetylated O-antigen of the SMH12 polysaccharide O-antigen. (a–c) the major conformation around the Man1→4Gal disaccharide moiety is shown, with two perspectives of the solvent-exposed surface for the saccharidic chain; (d–f) the same information, but by using the minor conformer around the Man→Gal fragment.

Conclusions

The solution conformation and dynamic features of the deacetylated O-antigen of *S. fredii* SMH12 was elucidated by using a variety of NMR spectroscopic and molecular mechanics calculations. It was shown that the polysaccharide displays a variety of internal motions around the glycosidic linkages, with distinct flexibility depending on the nature of the glycosidic linkage. Indeed, the Manα1→4Gal is strikingly much more flexible than the alternative Gal1→3Rha and Rha1→3Man linkages, at least for this polysaccharide.

Experimental Section and Computational Details

The O-antigen was isolated and its composition identified as described previously.[6]

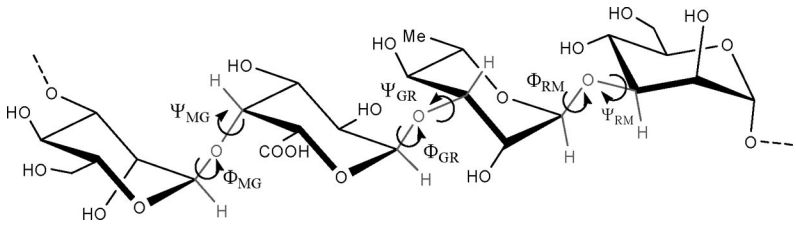

Scheme 1. Definition of the key torsion angles of the trisaccharide repeating unit of the O-antigen.

NMR Spectroscopy:[12] Samples were deuterium exchanged several times by freeze-drying from ^2H_2O, and then examined in solution (5 mg/750 μL) in 99.98% ^2H_2O. Spectra were recorded at 303 K with a Bruker AV500 spectrometer operating at 500.13 MHz (^1H) and 125.75 MHz (^{13}C). Chemical shifts are given in ppm by using the ^{2}HHO signal (δ = 4.75 ppm) (^1H) and external dimethyl sulfoxide (δ = 39.5 ppm) (^{13}C) as references. The TOCSY was acquired by using a data matrix of 256 × 2 K points to digitize a spectral width of 4084 Hz; 16 scans per increment and an isotropic mixing time of 90 ms were used. The 2D homonuclear DQF-COSY was performed by using the Bruker standard pulse sequence. A data matrix of 256 × 2 K points was used to digitize a spectral width of 3280 Hz; 16 scans were used per increment. The 2D heteronuclear one-bond proton–carbon correlation experiment was registered in the ^1H-detection mode by single-quantum coherence (HSQC). A data matrix of 256 × 1 K points was used to digitize a spectral width of 3280 and 22522 Hz in F_2 and F_1; 64 scans were used per increment. ^{13}C decoupling was achieved by the GARP scheme. Squared–cosine–bell functions were applied in both dimensions, and zero filling was used to expand the data to 512 × 1 K. This experiment was slightly modified by the implementation of an editing block in the sequence.[13] The HMBC experiment was performed by using the Bruker standard sequence with 256 increments of 1 K real points to digitize a spectral width of 4084 × 30030 Hz; 64 scans were acquired per increment with a delay of 70 ms for evolution of long-range couplings. The coupled HSQC one-bond proton–carbon correlation experiment was registered in the ^1H-detection mode by single-quantum coherence. A data matrix of 256 × 2 K points was used to digitize a spectral width of 2694 and 22522 Hz in F_2 and F_1; 48 scans were used per increment. Squared-cosine-bell functions were applied in both dimensions, and zero filling was used to expand the data to 1 × 2 K. Pure absorption NOESY experiments was performed with mixing times of 100, 150, 200, and 250 ms. A data matrix of 256 × 2 K points was used to digitize a spectral width of 4084 Hz; 32 scans were used per increment.

Molecular Mechanics and Dynamics Simulations: The MD study was performed with an octasaccharide molecule defined as: α-D-Man*p*-(1→4)-α-D-Gal*p*A-(1→3)-α-L-Rha*p*-(1→3)-α-D-Man*p*-(1→4)-α-D-Gal*p*A-(1→3)-α-L-Rha*p*-(1→3)-α-D-Man*p*-(1→4)-α-D-Gal*p*A to properly consider the environment of the trisaccharide repeating unit.[14] The key torsional angles were defined as described in Scheme 1.

Φ_{MG} (ΦMan*p* – Gal*p*A): H-1(Man)-C-1(Man)-O-1–C-4(GalA)

Ψ_{MG} (ΨMan*p* – Gal*p*A): C-1(Man)-O-1–C-4(GalA)-H-4(GalA)

Φ_{GR} (ΦGal*p*A – Rha*p*): H-1(GalA)-C-1(GalA)-O-1–C-3(Rha)

Ψ_{GR} (ΨGal*p*A – Rha*p*): C-1(GalA)-O-1–C-3(Rha)-H-3(Rha)

Φ_{RM} (ΦRha*p* – Man*p*): H-1(Rha)-C-1(Rha)-O-1–C-3(Man)

Ψ_{RM} (ΨRha*p* – Man*p*): C-1(Rha)-O-1–C-3(Man)-H-3(Man)

The calculations were performed by using the MM3* as integrated in the Maestro package[15] by using the GB/SA (generalized born solvent-accessible surface area) to simulate the water environment.[16]

The starting structure was built by defining every Φ angle to the expected *exo*-anomeric[17] orientation (Φ_{MG} = –60°, Φ_{GR} = –60° y Φ_{RM} = 60°), whereas all Ψ values were initially set to 0°. This structure was then minimized by using a conjugate gradient protocol until convergence was obtained (energy difference of 0.05 kJ Å^{-1} mol^{-1}). Then, the minimized structure was employed as starting structure for MD simulations at 300 K by using the same force field, MM3*. The integration step was 1 fs. Snapshots were saved every 8 ps, with a total simulation time of 3 ns. The structures obtained through the MD simulations were then taken for simulating the theoretical NOESY spectra by using home-written software, which is available from the authors upon request.[18] Basically, all the positions of the protons of the MD-sampled octasaccharide moieties were considered. Different correlation times were considered to get the best fit between the observed and expected NOEs.[19]

A final MD run was also performed for the native acetylated molecule. The global minimum found for the deacetylated polysaccharide was modified by setting the corresponding acetyl and methyl groups at the proper positions and a new 3 ns MD simulation was launched. Snapshots were saved every 3 ps, and the results were compared to those acquired for the deacetylated derivative.

Supporting Information (see footnote on the first page of this article): Chemical shifts of the O-antigen; HSQC, TOCSY, and NOESY (150 ms) spectra of the deacetylated O-antigen of *S. fredii* SMH12.

Acknowledgments

The work was supported by the Ministerio de Ciencia y Tecnología (CTQ2006-10874-C02-01, AGL2005-07923-C05, and AGL2006-13758-C05) and the Junta de Andalucía (Grupo CVI0135). F. J. F. de C. was supported by a fellowship from Ministerio de Ciencia y Tecnología.

[1] P. van Berkum, B. D. Eardy in *The Rhizobiaceae: Molecular Biology of Model Plant–Associated Bacteria* (Eds: H. P. Spaink, A. Kondorosi, P. J. J. Hooykaas), Kluwer Academic Publishers, Dordrecht, The Netherlands, **1998**, pp. 1–24.

[2] B. R. Day, J. T. Loh, J. Cohn, G. Stacey in *Prokariotic Nitrogen Fixation. A Model System for the Analysis of a Biological Process* (Ed.: E. W. Tripplett), Horizon Scientific Press, Norfolk, U. K., **2000**, pp. 385–415.

[3] A. Becker, A. Pühler in *The Rhizobiaceae: Molecular Biology of Model Plant–Associated Bacteria*, (Eds: H. P. Spaink, A. Kondorosi, P. J. J. Hooykaas), Kluwer Academic Publishers, Dordrecht, The Netherlands, **1998**, pp. 97–118.

[4] N. Fraysse, F. Couderc, V. Poinsot, *Eur. J. Biochem.* **2003**, *270*, 1365–1380.

[5] E. L. Kannenberg, B. L. Reuhs, L. S. Fosberg, R. W. Carlson in *The Rhizobiaceae: Molecular Biology of Model Plant–Associated Bacteria* (Eds: H. P. Spaink, A. Kondorosi, P. J. J. Hooykaas), Kluwer Academic Publishers, Dordrecht, The Netherlands, **1998**, pp. 119–154.
[6] F. J. Fernández de Córdoba, M. A. Rodríguez-Carvajal, P. Tejero-Mateo, J. Corzo, A. M. Gil-Serrano. *Biomacromolecules*, DOI: 10.1021/bm701011d.
[7] For studies on conformation and dynamics of oligo- and polysaccharides, see for instance: A. Almond, J. Duus, *J. Biomol. NMR* **2001**, *20*, 351–363.
[8] a) T. J. Rutherford, J. Partridge, C. T. Weller, S. W. Homans, *Biochemistry* **1993**, *32*, 12715–12724; b) A. Almond, J. Bunkenborg, T. Franch, C. H. Gotfredsen, J. O. Duus, *J. Am. Chem. Soc.* **2001**, *123*, 4792–4802.
[9] For instance, see: a) R. Stenutz, P. E. Jansson, G. Widmalm, *Carbohydr. Res.* **1998**, *306*, 11–17; b) P. E. Jansson, L. Kenne, T. Wehler, *Carbohydr. Res.* **1987**, *166*, 271–282; c) P. E. Jansson, L. Kenne, E. Schweda, *J. Chem. Soc. Perkin Trans. 1* **1987**, 377–383.
[10] D. Neuhaus, M. P. Williamson in *The Nuclear Overhauser Effect in Structural and Conformational Analysis*, Wiley-VCH, New York, **1989**.
[11] -For easy generation and analysis of potential energy maps of disaccharide entities, see: http://www.glycosciences.de/modeling/glycomapsdb.
[12] J. Jiménez-Barbero, T. Peters in *NMR Spectroscopy of Glycoconjugates* (Eds: J. Jiménez-Barbero, T. Peters), Wiley-VCH, Weinheim, **2002**.
[13] T. Parella, F. Sanchez-Ferrando, A. Virgili, *J. Magn. Reson.* **1997**, *126*, 274–277.
[14] S. Perez, A. Imberty, S. Engelsen, J. Gruza, K. Mazeau, J. Jiménez-Barbero, A. Poveda, J. F. Espinosa, B. van Eyck, G. Jonhson, A. French, M. Kouwijzer, D. Grootenhuis, A. Bernardi, L. Raimondi, H. Senderowitz, V. Durier, G. Vergoten, K. Rasmussen, *Carbohydr. Res.* **1998**, *314*, 141–155.
[15] N. L. Allinger, Y. H. Yuh, J. H. Lii, *J. Am. Chem. Soc.* **1989**, *111*, 8551–8566.
[16] W. C. Still, R. C. Tempczyk, R. C. Hawley, T. Hendrickson, *J. Am. Chem. Soc.* **1990**, *112*, 6127–6129.
[17] J. L. Asensio, F. J. Cañada, A. Garcia-Herrero, M. T. Murillo, A. Fernandez-Mayoralas, B. A. Johns, J. Kozak, Z. Zhu, C. R. Johnson, J. Jiménez-Barbero, *J. Am. Chem. Soc.* **1999**, *121*, 11318–11329.
[18] M. Martin-Pastor, J. L. Asensio, J. Jiménez-Barbero, *Int. J. Biol. Macromol.* **1995**, *17*, 137–148.
[19] A. Poveda, J. L. Asensio, M. Martin-Pastor, J. Jiménez-Barbero, *J. Biomol. NMR* **1997**, *10*, 29–43.

Received: February 18, 2008
Published Online: June 3, 2008

